J Membrane Biol (2015) 248:67–81
DOI 10.1007/s00232-014-9742-0

HCN2 Channels: A Permanent Open State and Conductance Changes

François Pittoors · Pierre Paul Van Bogaert

Received: 11 April 2014 / Accepted: 30 September 2014 / Published online: 13 November 2014

Abstract Hyperpolarization-activated cyclic nucleotide-gated (HCN) channels in the membranes of heart and brain cells can conduct Na^+ and K^+ ions and activate between −30 and −120 mV. We express the α subunit of HCN2 channels in *Xenopus laevis* oocytes and are confronted with two unexpected problems. First, we observe a rise in membrane conductance at resting potential proportional to the amount of expression. On activation to hyperpolarizing potentials, the instantaneous conductance rises in proportion to the amount of activated current. CsCl reduces the observed effects. This can be explained by the expression in oocytes membranes of a fraction of permanently open HCN2 channels. Second, using TEVC technique, our data show a completely different behaviour in physiological solutions of heterogeneously expressed HCN2 currents from what is observed in wild-type currents in the absence of drugs. During pulse trains, we frequently observe (1) a fast and significant decline of the amplitude of HCN2 current during hyperpolarizing steps, (2) no recovery of this decline after a long period at resting membrane potential, (3) a different behaviour of the tail currents at depolarization with other and slower changes than during activation, (4) recovery of this decline in high K^+/low Na^+ bath solution. The decline of the HCN2 current in physiological conditions is caused by a reduction of the conductance of the HCN2 channel presumably caused by the mere presence of sodium in the channel, in competition with potassium ions and with a limitative effect on the channel conductance.

F. Pittoors · P. P. Van Bogaert (✉)
Laboratory for Electrophysiology, Department of Cardiology, Institute Born-Bunge, University of Antwerp, Universiteitsplein 1, 2610 Antwerp, Belgium
e-mail: pp.vanbogaert@uantwerpen.be

Keywords HCN2 channels · *Xenopus laevis* oocytes · Channel permanent open state · Channel conductance changes · Two-electrode voltage clamp

Introduction

Although in our experiments the basic hyperpolarization-activated cyclic nucleotide-gated (HCN) currents show properties comparable to those expressed in *Xenopus laevis* oocytes published by other groups (Santoro et al. 1998; Chen et al. 2000, 2001a, b; Ulens and Tytgat 2001a, b; Yu et al. 2001; Xue and Li 2002; Xue et al. 2002; Azene et al. 2003; Decher et al. 2003; Henrikson et al. 2003; Lesso and Li 2003; Decher et al. 2004; Azene et al. 2005a, b; Cheng et al. 2007), some properties diverge from HCN currents described in the same expression system and from the pacemaker (I_f) currents described in native cells.

One observation is that, contrary to native I_f currents, a fraction of the steady-state-activated HCN current shows permanent activation at voltages positive to –60 mV. This has been observed and described in detail for HCN2 channels expressed in CHO-K1 cells (Macri et al. 2002; Proenza et al. 2002a, b; Macri and Accili 2004), in HEK 293 cells (Proenza and Yellen 2006), and in *X. laevis* oocytes expressing mutated channels (Chen et al. 2001a).

The second unexpected finding appears when voltage-clamp pulses between −30 and −120 mV are applied in trains to repetitively activate the HCN2 current. We observe (1) a fast and significant decline at hyperpolarization of the peak amplitude of the activated HCN2 current ($I_{HCN2,act}$), associated with a small slowing of the current's activation ($\tau_{HCN2,act}$), (2) no recovery of this decline after a long period at membrane resting potential (E_{rest}), (3) a different behaviour of the amplitude of HCN2

tail current at depolarization ($I_{HCN2,tail}$) with other and slower changes than at activation, (4) a faster and more pronounced decline of $I_{HCN2,act}$ in ND96 than in high K^+ bath solution, (5) a complete recovery of the decline from pulses in ND96 during pulses in high K^+/low Na^+ bath solution. The decline appears to be independent of the voltage clamp pulse protocol. This observation was never made in control conditions in SA node cells of rabbits (Bosmith et al. 1993; Goethals et al. 1993; DiFrancesco 1994; Bois et al. 1996; Bucchi et al. 2002), in DRG neurons (Raes et al. 1998), in sheep cardiac Purkinje fibres (Van Bogaert and Goethals 1987; Van Bogaert et al. 1990; Van Bogaert and Pittoors 2003), and in HCN1, HCN2, HCN3, and HCN4 expressed in HEK 293 CHO cells (Stieber et al. 2006; Thollon et al. 2007). In these native cardiac and neuronal cells, the amplitude of the HCN current remains constant during a train of voltage clamp pulses.

Although there is great variability in the occurrence of these events, we cannot neglect them, because our data show frequently and reproducibly a completely different behaviour of heterogeneously expressed HCN2 currents to what is observed with similar voltage clamp protocols with wild HCN currents in sheep cardiac Purkinje fibres, DRG cells, isolated sinus node cells, and heterologous-expressed HCN channels in HEK 293 cells.

Materials and Methods

Oocytes

We use wild *X. laevis* imported from South Africa by two different providers (Centre d'élevage de Xénopes, CNRS, Montpellier, France and Xenopus Express France, 43270 Vernassal, Haute-Loire, France). Ovarian tissue is removed surgically after anaesthesia of the animals in ice-cold water for 45 min and ice-cold 0.1 % Tricaine (ethyl 3-amino-benzoate methane sulphonate salt) solution for another 45 min. Oocyte defolliculation is performed by treatment with collagenase (Liberase Blendzyme 3, Roche: collagenase Wünsch units 0.5 U ml^{-1}) in Ca^{++}-free ND96 solution at room temperature for 90 min until dissociation (Colville and Gould 1994; Smart and Krishek 1995). We select mature oocytes stage 5 and 6 which have a diameter between 1.0 and 1.3 mm (Brown 2004). After injection of 50 ng mRNA (1 ng nl^{-1}) of HCN2 (α subunit), we store the cells at 11 °C in ND96 with addition of Gentamicin sulphate 100 µg ml^{-1}, Penicillin 100 Units ml^{-1}, and Streptomycin 100 µg ml^{-1} (Eidne 1994). We perform the experiments at room temperature. The cells are laid in an oocytes chamber (RC-3Z Oocyte Recording Chamber, Warner Instruments; volume 0.5 ml). The solution flows into the chamber by gravity at a rate of 2 ml min^{-1}. Injected cells can be used for 8 days.

HCN2 Origin

We have injected cRNA from two different sources.

Our first cDNA construct (originally termed mBCNG-2) is a generous gift of Dr. Steven A. Siegelbaum Ph.D. (Department of Pharmacology, Columbia University, New York) to Prof Jan Tytgat (Laboratory of Toxicology, University of Leuven) who performed the in vitro transcription: the entire coding sequence for the mouse HCN2 channel was subcloned into the vector pGEMHE. Plasmid was first linearized with SphI. Next, the cRNA was synthesised from the linearized plasmid using the large scale T7 mMessage mMachine transcription kit (Ambion). The same cRNA is used by other groups (Ulens and Tytgat 2001b; Yu et al. 2001; Xue and Li 2002).

The second cDNA construct and in vitro transcription were performed by Dr. Alain Labro (Laboratory of molecular biophysics, physiology and pharmacology, University of Antwerp): total RNA and subsequently messenger mRNA were isolated from mouse brain using TRIzol Reagent (Invitrogen, San Diego, CA, USA) and Poly(A)Purist isolation kit (Applied Biosystems, Foster City, CA, USA). Isolated mRNA was reversed transcribed with the Thermoscrips RT-PCR System (Invitrogen) using random hexamer primers. mHCN2 cDNA was amplified in a PCR reaction with gene-specific primers, the high fidelity polymerase *TaKaRa LA Taq* (Takara Bio Inc, Otsu, Shiga, Japan), and 10 % DMSO. Amplified fragments were cloned into the TOPO-TA vector (Invitrogen), and double-strand sequencing confirmed the identity of the obtained clone with the original described mHCN2 sequence (originally named mBCNG-2) (Santoro et al. 1998). Subsequently, the entire coding sequence for the mHCN2 channel was subcloned into the vector pSP64 Poly(A) (Promega, Madison, WI, USA) for in vitro mHCN2 cRNA synthesis. Plasmid DNA was amplified in XL2 blue script cells (Stratagene, La Jolla, CA, USA) and harvested using the GenElute HP plasmid maxiprep kit (Sigma-Aldrich, St. Louis, MO, USA). Double-strand sequencing confirmed the correctness of the mHCN2-pSP64 Poly(A) construct. Plasmids were linearized with the enzyme *Pvu*II and afterward purified with GenElute PCR Clean-Up kit (Sigma-Aldrich). Next, the cRNA was synthesised from the linearized plasmids using the large scale SP6mMessage mMachine transcription kit (Applied Biosystems).

Bath Solution

Most experiments are performed either in high Na^+/low K^+ bath solution (ND96) or in high K^+/low Na^+ bath

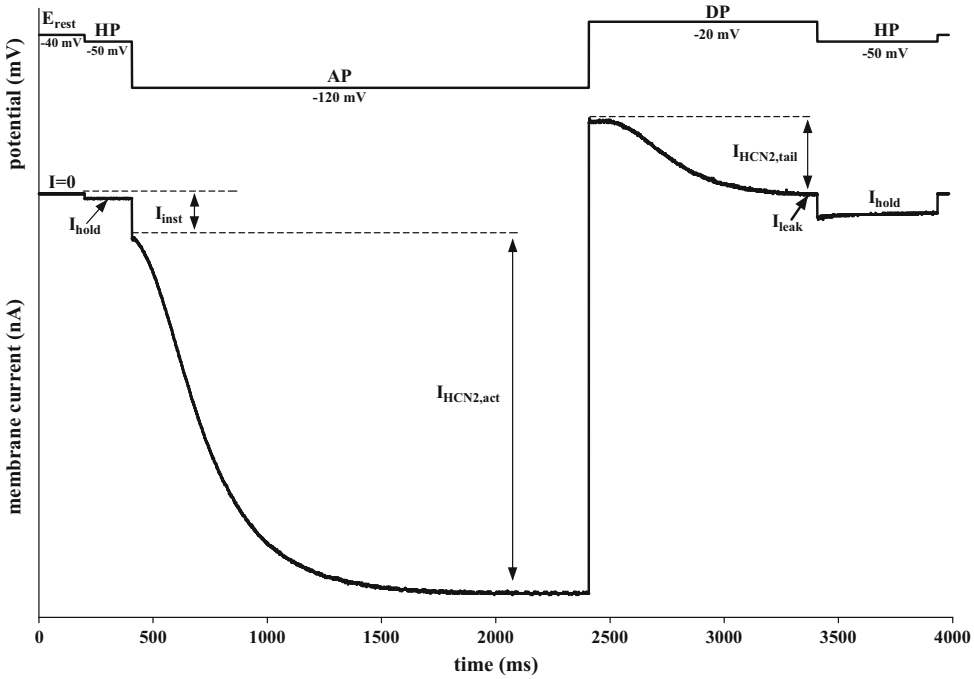

Fig. 1 TEVC test pulse protocol and subsequent current response. From a holding potential (HP) with subsequent holding current (I_{hold}), we apply a hyperpolarizing voltage pulse (AP) and measure instantaneous current (I_{inst}) and activated current ($I_{HCN2,act}$). After the HCN2 current has reached a stable value, the membrane potential is clamped to a variable voltage (DP) where the current deactivates. We measure tail current ($I_{HCN2,tail}$) and residual leak current (I_{leak}). Biophysical terms are indicated

solution. ND96:NaCl 96 mM, KCl 2 mM, $CaCl_2$ 1.8 mM, $MgCl_2$ 1 mM, HEPES 5 mM, NaOH at pH 7.4 (about 2 mM), osmolarity 198 mOsm; high K^+/low Na^+ solution: NaCl 2 mM, KCl 96 mM, $CaCl_2$ 1.8 mM, $MgCl_2$ 1 mM, HEPES 5 mM, KOH at pH 7.4 (about 2 mM), osmolarity 198 mOsm. The intracellular ion concentrations in large oocytes defolliculated by collagenase differ in different studies (Dascal 1987; Costa et al. 1989; Weber 1999). We take the values from Costa: 10.1 mM for Na^+, 109.5 mM for K^+ and 37.7 mM for Cl^-. Using the Nernst equation, we calculate the Nernst equilibrium potential for the different ions in oocytes. In ND96 at 22 °C: $E_{Na} = +57.8$ mV, $E_K = -101.8$ mV, and $E_{Cl} = -25.8$ mV. We are aware that in low Na^+ bath solutions the concentration of Na^+ in the cytoplasm will drop progressively as described in sheep cardiac Purkinje fibres (Deitmer and Ellis 1980) and in toad oocytes where Na^+ was replaced by Li^+ (Dick and McLaughlin 1969) and that E_{Na} can only be approximated. There are no published data about the Na^+ concentration in the cytoplasm of the oocyte bathed in high K^+/low Na^+ solution. In high K^+/low Na^+ solution at 22 °C (supposing stable inner concentrations): $E_{Na} \approx -41.2$ mV, $E_K = -2.8$ mV and $E_{Cl} = -25.8$ mV.

Microelectrodes

The microelectrodes for the potential measurement are filled with a 3 M KCl solution and have a mean resistance of 2.0 MΩ. The microelectrodes for the current injection are filled with a 0.8 M KCl + 1.6 M Tripotassium Citrate solution and have a mean resistance of 1.4 MΩ.

Voltage Clamp Amplifier And Software

We use a GeneClamp 500 amplifier with pClamp6 and later pClamp10 data acquisition software (Axon CNS, Molecular Devices, MDS Analytical Technologies). In TEVC mode, we insert a grounded shield between the two electrodes in order to reduce the capacitive crosstalk (Smart and Krishek 1995; Stamps and Begenisich 1998). We can set the gain of the amplifier to maximum (10 k) with a stability setting of 80–120 µS without generating oscillations. The measured current is filtered at 500 Hz, and the sampling frequency is 1 or 2 kHz.

Experimental Protocols

After impalement of the cell, we measure the membrane resting potential (E_{rest}).

With the TECC technique, we measure the change in the potential (ΔE_{cc}) and the exponential time constant (τ_{cc}) in order to calculate the membrane resistance (R_m) and capacity (C_m) at rest.

In TEVC condition, we apply a hyperpolarizing test pulse to activate the expressed HCN2 channels, followed by a depolarizing pulse to close the channels (Fig. 1).

Pulse train (PT) protocols consist of consecutive test pulses of 50–350 pulses.

Data Analysis

We never use leak subtraction.

The time courses of activation and deactivation of I_{HCN2} happen to follow a sigmoid time course (DiFrancesco 1985; Macri and Accili 2004). We determine (1) the amplitude of the instantaneous current (I_{inst}) and activated HCN2 current ($I_{HCN2,act}$) at hyperpolarization and tail HCN2 current ($I_{HCN2,tail}$) and leak current (I_{leak}) at depolarization, (2) the exponential time constant of activation ($\tau_{HCN2,act}$) and of deactivation ($\tau_{HCN2,tail}$).

We evaluate the potential of half-open probability of HCN2 channels ($V_{1/2}$) and slope in ND96 using the Boltzmann equation:

$$P_0 = \frac{1}{1 + e^{-\left(\frac{V - V_{1/2}}{slope}\right)}}. \quad (1)$$

We refrain from calculating the minimum open probability (min-P_{open}) due to the presence of permanently open HCN2 channels by subtracting the mean leak current as is done by other groups (Chen et al. 2001a; Proenza et al. 2002a; Xue and Li 2002; Xue et al. 2002; Azene et al. 2003; Henrikson et al. 2003; Lesso and Li 2003; Decher et al. 2004; Azene et al. 2005a, b; Proenza and Yellen 2006; Cheng et al. 2007; Au et al. 2008), because the leak current measured in uninjected cells exhibits a large variation at −20 mV $I_{leak,0}$ = 7 nA (SD = 21 nA, n = 46).

We evaluate the reversal potential of the HCN2 current (E_{HCN2}) with fully activated current–voltage relations. The fully activated current–voltage relations diverge slightly from linearity (Hestrin 1987; Moroni et al. 2000; Macri and Accili 2004; see discussion).

All conductances (G) are normalized to the membrane surface by division by the membrane capacity. N_{HCN2} is the number of expressed channels, P_o is the open probability and γ_{HCN2} is the single channel conductance of the HCN2 channel.

We define $G_{HCN2} = N_{HCN2} \times P_o \times \gamma_{HCN2}$, $G_{Na} = N_{HCN2} \times P_o \times \gamma_{Na}$, $G_K = N_{HCN2} \times P_o \times \gamma_K$.

The ratio of the individual conductance of Na^+ (G_{Na}) and K^+ (G_K) in the HCN2 channel can be calculated as

$$\frac{G_{Na}}{G_K} = -\frac{E_{HCN2} - E_K}{E_{HCN2} - E_{Na}}. \quad (1)$$

Results

A Permanent Open State

No Expression of HCN2 ($I_{HCN2,act}$ = 0, Subscript 0)

We measure the mean membrane resting potential ($E_{rest,0}$) and the conductance at membrane resting potential ($G_{m,0}$) in uninjected cells (n = 124), cells injected with water (n = 11), and cells injected with mHCN2 but without expression (n = 65). These are considered as wild cells. There appears to be no difference between uninjected cells and cells injected with water or mHCN2 but without expression. We conclude that injection does not induce leakage in the cells.

In these cells, $E_{rest,0}$ = −44.7 mV (SD = 11.0 mV, n = 124) and $G_{m,0}$ = 0.0055 µS nF^{-1} (SD = 0.0033 µS nF^{-1}, n = 124), which corresponds with a membrane resistance of 1.03 MΩ.

In voltage clamp conditions, the conductance at the onset of the hyperpolarization ($G_{inst,o}$) is also a measure for the amount of permanently open channels, as no activation of time-dependent channels has yet taken place. $G_{inst,0}$ = 0.0096 µS nF^{-1} (SD = 0.0068 µS nF^{-1}, n = 124).

With Expression of HCN2 Channels (Subscript 1)

Open Probability (P_{open}) and Reversal Potential (E_{HCN2})

From steady-state activation curves on cells with expression of mHCN2, we calculate $V_{1/2}$ = –64.4 mV (SD = 8.0 mV, n = 40) and the slope = −5.5 mV (SD = 1.6 mV, n = 40).

From fully activated current–voltage relations, we calculate E_{HCN2} = −32.5 mV (SD = 8.7 mV, n = 158).

Before Any Activation of HCN2

Membrane resting potential ($E_{rest,1}$) is less negative in cells with expression compared to cells without expression. There is an exponential correlation between E_{rest} and G_{act} : $\left[E_{rest,1} = E_{rest,0} + \left(E_{HCN2} - E_{rest,0}\right) \times \left(1 - e^{-Gact/c}\right)\right]$: r = 0.330, $E_{rest,0}$ = −43.1 mV corresponding to G_{act} = 0 (no expression) and E_{HCN2} = –32.3 mV corresponding to $G_{act} = \infty$ (very high expression); c = 0.245 µS nF^{-1}. This suggests that $E_{rest,1}$ shifts from $E_{rest,o}$ (no expression) toward E_{HCN2} in proportion to the expression of HCN2 channels (Fig. 2).

The conductance at membrane resting potential in cells with expression is $G_{m,1}$ = 0.0324 µS nF^{-1} (SD = 0.0411 µS nF^{-1}, n = 390). It is clear that the average of G_m in the two populations (uninjected versus with expression) is different ($p < 0.05$) and that the large standard deviation in cells with expression is due to the very large range of expression.

At Activation of HCN2

$G_{inst,1}$ is a measure for the amount of all permanently open channels, because at the onset of the hyperpolarization no activation of HCN2 has yet taken place. $G_{inst,1}$ = 0.0576 µS nF^{-1} (SD = 0.0708 µS nF^{-1}, n = 390).

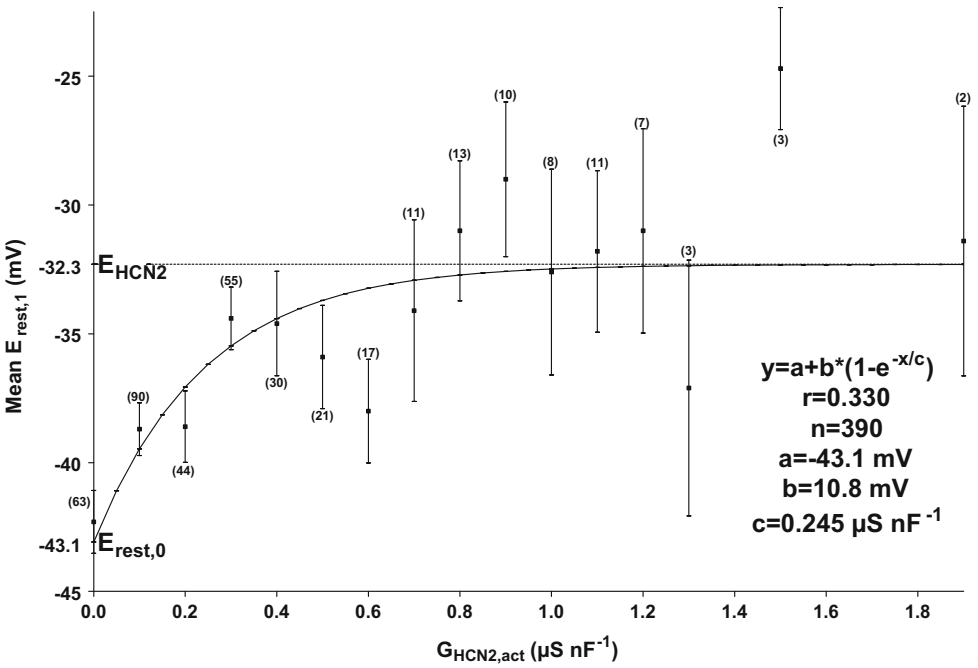

Fig. 2 Exponential correlation between $G_{HCN2,act}$ and $E_{rest,1}$. $G_{HCN2,act}$ has been rounded off (1) and means of $E_{rest,1}$ are plotted with SD and n. There is a medium correlation between the two parameters ($r = 0.330$). For $G_{HCN2,act} = 0$ (no expression), the value of $E_{rest,1}$ corresponds with $E_{rest,0}$ (−43.1 mV). For $G_{HCN2,act} = \infty$, the value of $E_{rest,1}$ corresponds with the reversal potential of the HCN2 current E_{HCN2} (−32.3 mV)

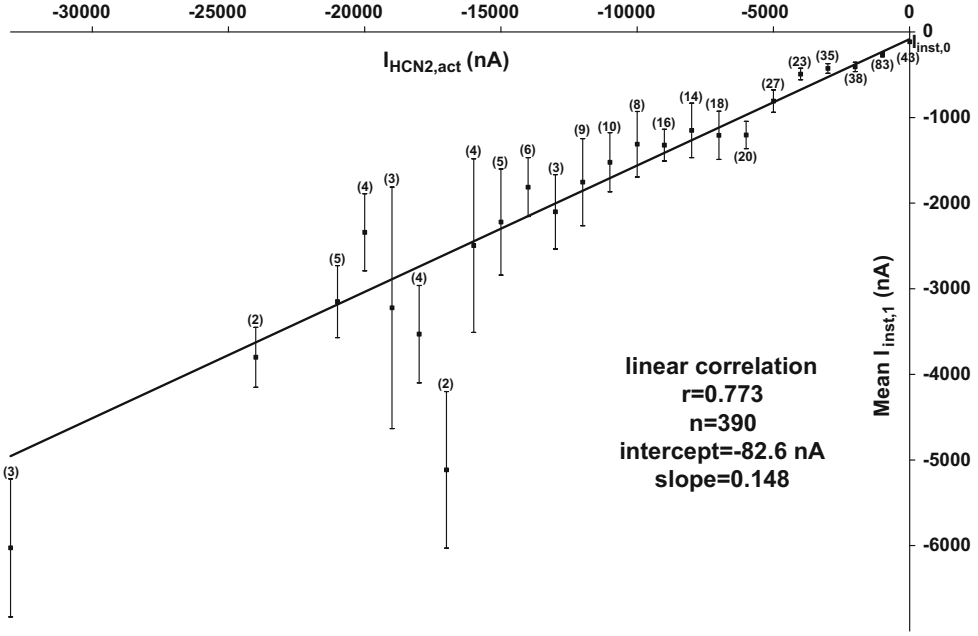

Fig. 3 Correlation between $I_{HCN2,act}$ and $I_{inst,1}$. $I_{HCN2,act}$ has been rounded off (−3) and means of $I_{inst,1}$ are plotted with SD and n. A strong linear correlation exists between these two parameters ($r = 0.773$). The intercept (−82.6 nA) corresponds with $I_{inst,0}$ (no expression). The slope (0.148) is an estimation for the fraction of permanently open channels co-expressed with voltage-activated HCN2 channels: the ratio of permanently open to activated channels is 0.148. The fraction of expressed channels in a permanently open state is then 12.9 %

The activated current ($I_{HCN2,act}$) is a measure of the amount of HCN2 channel expression but is function of the command potential. As the instantaneous current ($I_{inst,1}$) at the onset of hyperpolarization and the time-dependent $I_{HCN2,act}$ are measured at the same activation potential (AP), we can evaluate their correlation. We record higher $I_{inst,1}$ when $I_{HCN2,act}$ is greater with a strong linear correlation between the two parameters (Fig. 3).

The intercept at $I_{HCN2,act} = 0$ gives an estimation of $I_{inst,0}$ (cells without expression) and is consistent with our data.

$G_{HCN2,act}$ is the conductance of the HCN2 channels at potentials where the maximum amount of channels has been activated. There is a strong linear correlation between $G_{HCN2,act}$ and $G_{inst,1}$: $r = 0.764$ (Fig. 4).

After Depolarization

At the end of the depolarization, all HCN2 channels are supposed to be closed and only the current through other permanently open channels should remain. $G_{leak,1}$ reflects

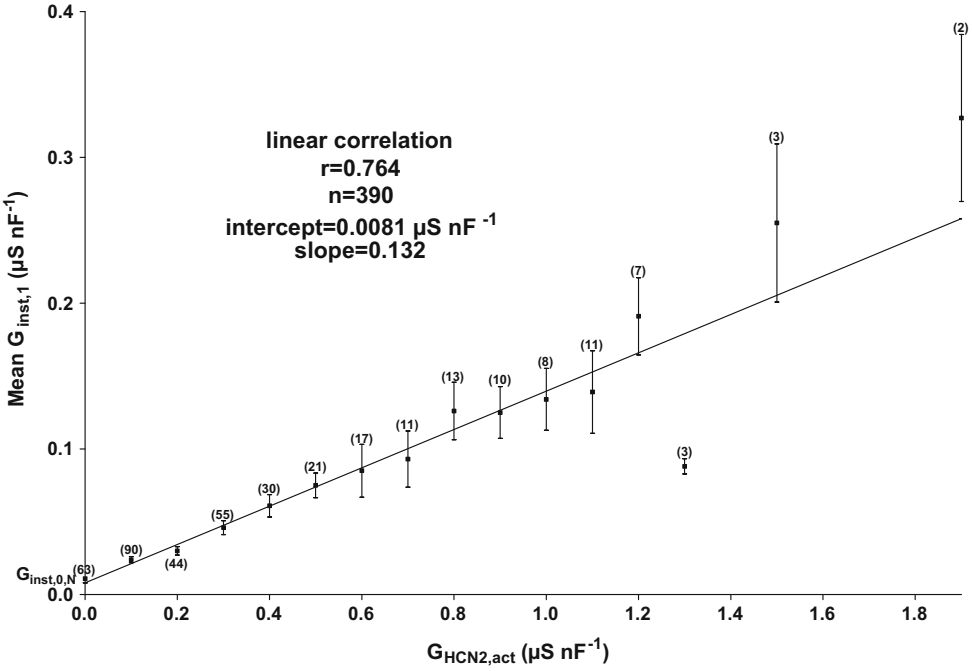

Fig. 4 Correlation between $G_{HCN2,act}$ and $G_{inst,1}$. $G_{HCN2,act}$ has been rounded off (1) and means of $G_{inst,1}$ are plotted with SD and n. A strong linear correlation exists between these two parameters ($r = 0.764$). The intercept (0.0081 µS nF^{-1}) corresponds with $G_{inst,0}$ measured in cells without expression. The slope (0.132) is a measure for the amount of permanently open channels co-expressed with voltage-activated HCN2 channels. From the slope, we calculate that 11.7 % of the expressed channels are in a permanently open state. This estimation matches with the result in Fig. 3

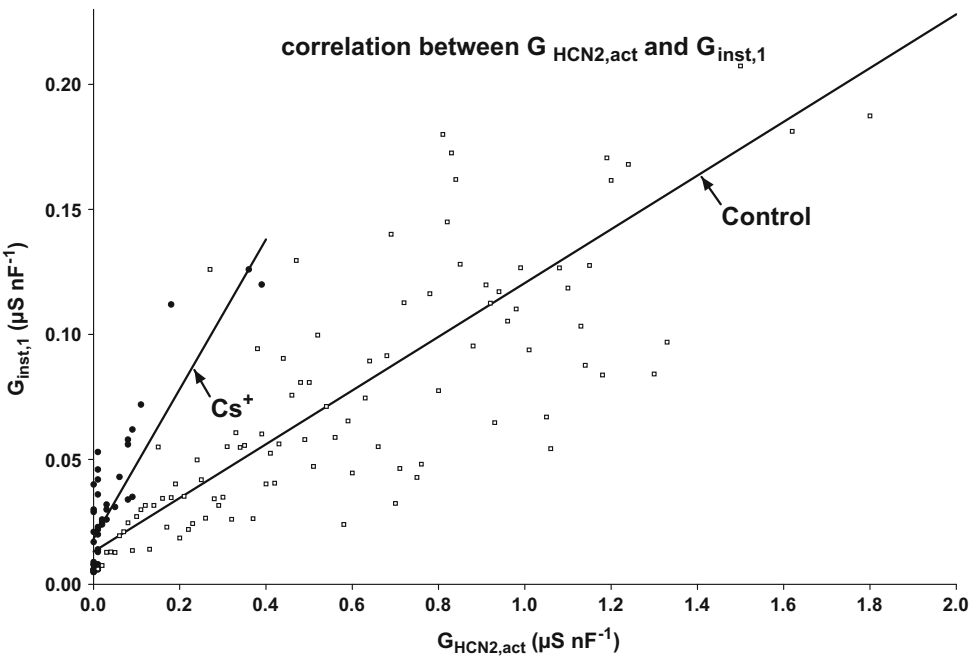

Fig. 5 Effect of Cs^+ on $G_{inst,1}$. Plot of the correlation between $G_{HCN2,act}$ and $G_{inst,1}$ in control conditions (ND96) and after addition of CsCl (2 mM) to the bath solution (Cs^+). In the two sets of results, a strong linear correlation exists between these two parameters. $G_{HCN2,act}$ is blocked for 92 % but $G_{inst,1}$ is less blocked (46 %), which is expressed by a rise in the slope. The permanently open channels co-expressed with voltage-activated HCN2 channels are less sensitive to block by Cs^+. The intercept is nearly the same in the two conditions and is an approximation of $G_{inst,0}$ (no expression)

the sum of the conductance through the leak channels in uninjected wild cells ($G_{leak,0}$) and the permanently open channels expressed together with HCN2 channel ($G_{HCN2,po}$). There exists a clear linear correlation between $G_{leak,1}$ and $G_{HCN2,act}$: $r = 0.739$.

Experiments with Block of $I_{HCN2,act}$ by CsCl

After addition of 2 mM Caesium Chloride (Cs^+) to the bath solution, the activated inward HCN2 current ($I_{HCN2,act}$) is almost totally blocked (DiFrancesco 1982). We apply a constant current pulse and a voltage clamp test pulse before and after addition of 2 mM Cs^+. $E_{rest,1}$ shifts to more negative values ($\mu = 16$ %, $n = 38$), and we note a decrease under influence of Cs^+ of $G_{m,1}$ ($\mu = 37$ %, $n = 57$), of $G_{inst,1}$ ($\mu = 46$ %, $n = 58$), and of $G_{HCN2,act}$ ($\mu = 92$ %, $n = 45$). $G_{m,1}$ and $G_{inst,1}$ decrease less than $G_{HCN2,act}$ under influence of Cs^+: at nearly total block of $G_{HCN2,act}$ only part of $G_{m,1}$ and $G_{inst,1}$ are blocked.

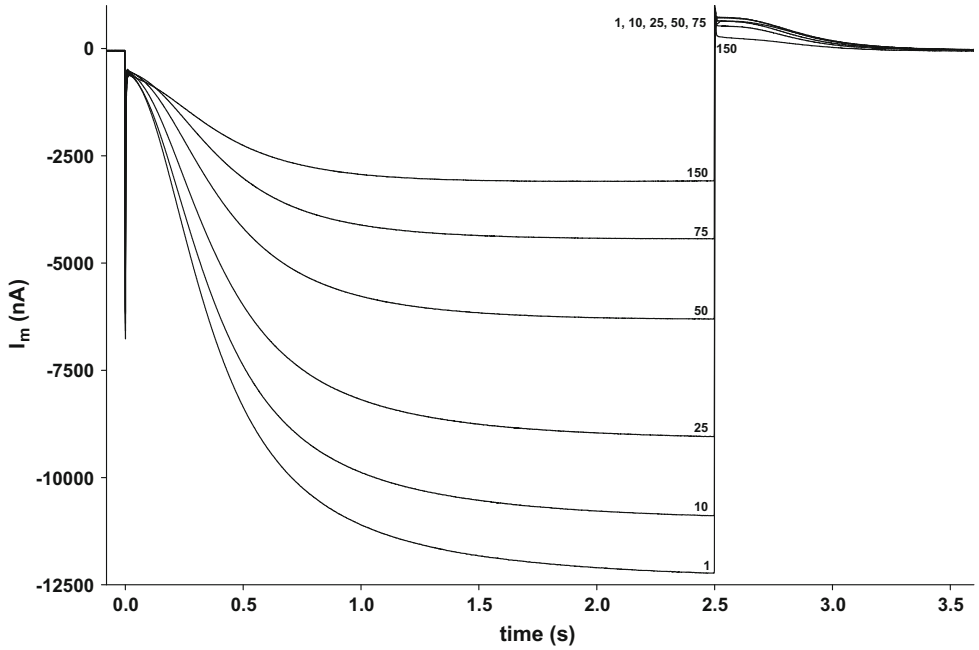

Fig. 6 Pulse train in ND96. Train of 150 pulses activating from −20 mV to −110 mV during 2,500 ms followed by deactivation to −20 mV during 7500 ms. $I_{HCN2,act}$ decreases 79 % while $I_{HCN2,tail}$ decreases 57 %. The decrease of $_{IHCN2,act}$ is faster (exponential time constant of 50 pulses) than the decrease of $I_{HCN2,tail}$ (exponential time constant of 80 pulses) which starts after a delay (at pulse 75 the major part of the decrease in $I_{HCN2,act}$ has taken place, where the decrease in $I_{HCN2,tail}$ has just begun). I_{inst} remains within 5 % of the initial value. Experiment 06 02 2009

The linear correlations between $G_{HCN2,act}$ and $G_{inst,1}$ in control and with Cs^+ have the same intercept ($G_{HCN2,act} = 0$, no expression) but the slope nearly triples after block of the HCN2 current with Cs^+ (Fig. 5).

Cs^+ blocks the activated HCN2 current for the greater part but blocks only partly the instantaneous current.

Apparent Use-Dependent Block

I_{HCN2} Changes During a Pulse Train in ND96

We perform 49 PT of 100 or 250 pulses in ND96 with one identical protocol: AP = −120 mV, AT = 1,000 ms, DP = −30 mV, and depolarization duration 1,560 ms.

In 10 PT, $I_{HCN2,act}$ is stable within 5 % of the initial value, but in 39 PT $I_{HCN2,act}$ decreases more than 5 % ($\mu = 0.30$, SD = 0.16).

In 17 PT, $I_{HCN2,tail}$ is stable within 5 % of the initial value, but in 9 PT $I_{HCN2,tail}$ increases more than 5 % ($\mu = -0.48$, SD = 0.46) while in 23 PT $I_{HCN2,tail}$ decreases more than 5 % ($\mu = 0.17$, SD = 0.14).

The $I_{HCN2,act}$ and the $I_{HCN2,tail}$ do not change in the same proportion nor with the same kinetic (Fig. 6).

The kinetic of decrease of the $I_{HCN2,act}$ during the PT is fast exponential in 30 cases ($\mu = 43$ pulses, SD = 53 pulses) but the kinetic of change of $I_{HCN2,tail}$ during a PT is mostly slow. The kinetic of activation of the HCN2 current itself ($\tau_{HCN2,act}$) slows down more than 5 % during the PT (increase of $\tau_{HCN2,act}$) in 26 experiments ($\mu = -0.38$, SD = 0.25) while in 17 experiments $\tau_{HCN2,act}$ accelerates more than 5 % ($\mu = 0.13$, SD = 0.04).

With other protocols, we also obtain in most cases a decrease of $I_{HCN2,act}$ and different changes in $I_{HCN2,tail}$. Altogether we perform 286 PT (different cells) in ND96.

To exclude a shift in the activation curve, we measured the steady-state HCN2 activation curve before and after a PT and evaluated the $E_{0.5}$ with a Boltzmann fit of the normalized tail currents (Fig. 7).

Although there is a clear decrease of the activated current after the PT, we observe no significant shift of the activation curve ($E_{0.5}$ control = −53 mV, $E_{0.5}$ after PT = −56 mV).

We evaluate in 28 additional experiments E_{HCN2} and G_{HCN2} (slope conductance at $i_{HCN2} = 0$) with fully activated current–voltage relations before and after a PT (Fig. 8).

For E_{HCN2}, we notice only a small shift to more positive values ($E_{HCN2,before}$: $\mu = -30.4$ mV, SD = 5.9 mV; $E_{HCN2,after}$: $\mu = -28.3$ mV, SD = 6.7 mV). For G_{HCN2}, we find an increase ($\mu = 17$ %) in 6 cases and a decrease in 22 cases ($G_{HCN2,before}$: $\mu = 51.7$ μS nF^{-1}, SD = 77.9 μS nF^{-1}; $G_{HCN2,after}$: $\mu = 28.4$ μS nF^{-1}, SD = 27.3 μS nF^{-1}).

The I_{inst} showed variable changes during the voltage clamp PT. There is no relation between the changes in

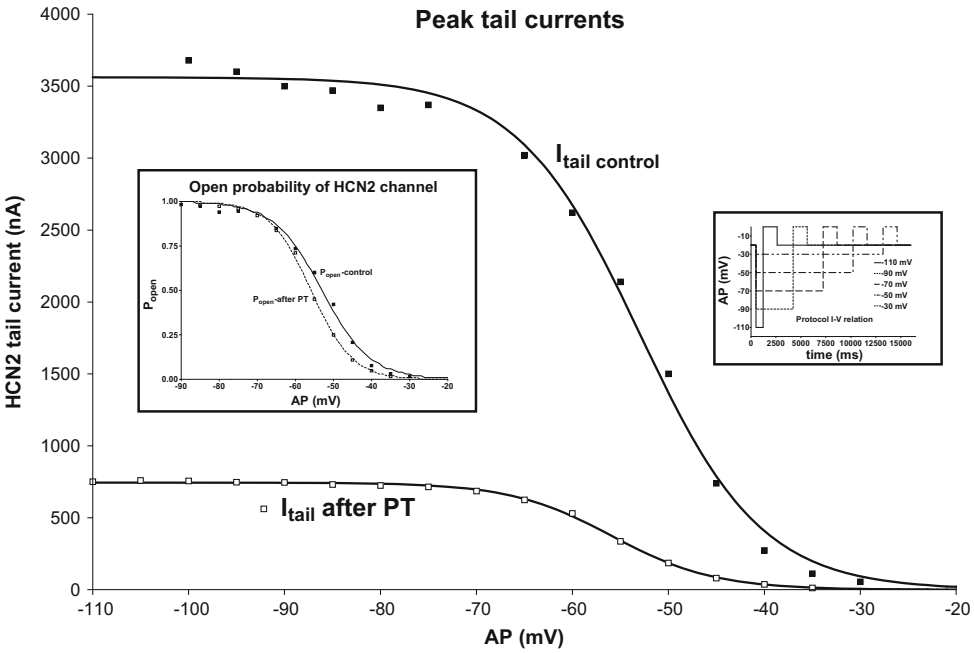

Fig. 7 Steady-state HCN2 activation curve before and after pulse train in ND96. Amplitude of the tail currents at 0 mV after steady-state activation at potentials ranging from −30 to −110 mV (see protocol in *inset*). The Boltzmann fit for the normalized tail currents yields $E_{0.5}$ control = −53 mV and $E_{0.5}$ after the PT = −56 mV (see *inset*). We notice a clear decrease in tail current amplitudes (79 %) after the PT without significant shift in open probability of the activated HCN2 channels

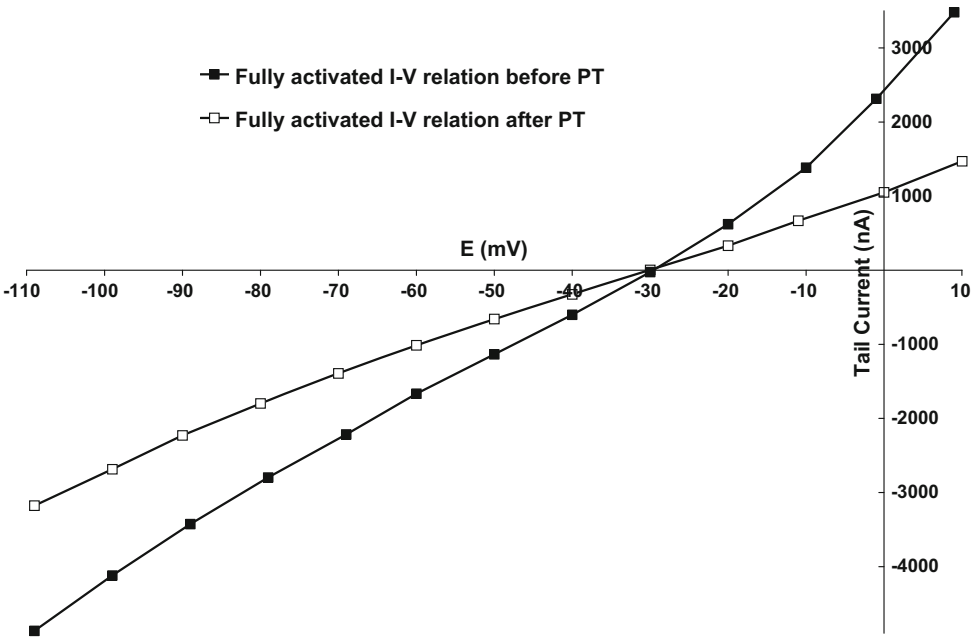

Fig. 8 Fully activated I–V relation before and after Pulse train in ND96. For E_{HCN2} we notice only a small shift to more positive values ($E_{HCN2,before}$: $\mu = -30.4$ mV, SD = 5.9 mV; $E_{HCN2,after}$: $\mu = -28.3$ mV, SD = 6.7 mV). For G_{HCN2} we find an increase ($\mu = 17$ %) in 6 cases and a decrease in 22 cases ($G_{HCN2,before}$: $\mu = 51.7$ μS nF^{-1}, SD = 77.9 μS nF^{-1}; $G_{HCN2,after}$: $\mu = 28.4$ μS nF^{-1}, SD = 27.3 μS nF^{-1})

$I_{HCN2,act}$ and $I_{HCN2,tail}$ on the one hand and I_{inst} on the other hand.

Test Pulse After a Pulse Train

In most cases, no recuperation of the initial conductance is obtained in ND96 after a period at E_{rest}. A test pulse, applied after the PT after more than 5 min at E_{rest} in the same bath solution, shows hardly any change of $I_{HCN2,act}$ and $I_{HCN2,tail}$ in comparison with the value at the end of the PT (Fig. 9).

Reversibility of Decline of $I_{HCN2,act}$

The observed decline of $I_{HCN2,act}$ is reversible. The following protocols demonstrate this crucial point.

In the first protocol, we started with a PT in high Na^+ solution followed by a second PT in high K^+ solution to

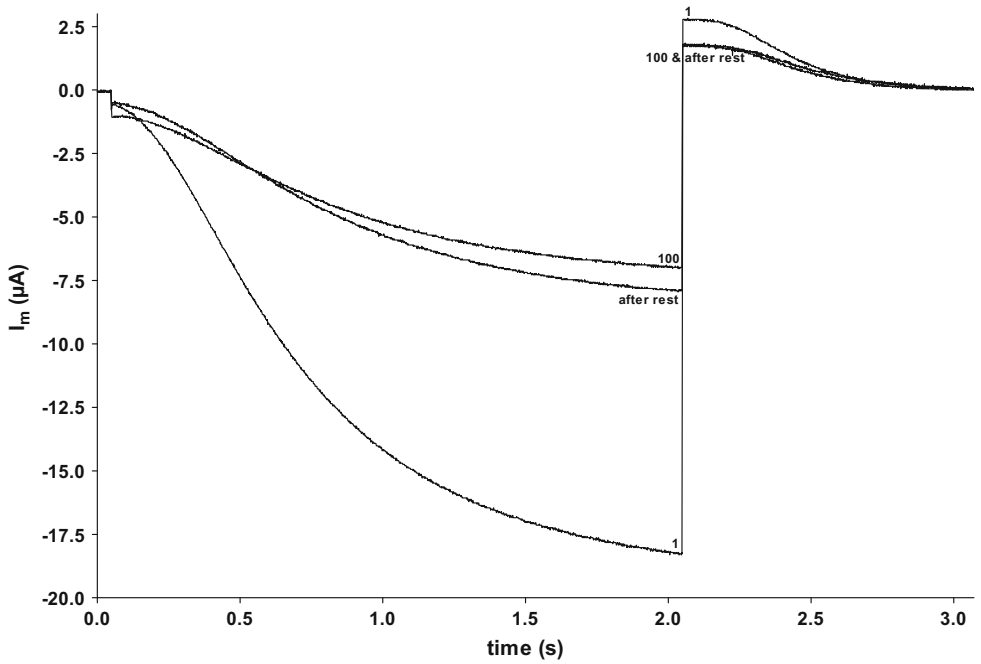

Fig. 9 Test pulse after a PT in ND96. After a PT of 100 pulses (pulse 1 and 100), the cell remains during 15 min at E_{rest} in the same bath solution ND96. Then we apply one test pulse (after rest) with the same parameters as in the PT. No recuperation of $I_{HCN2,act}$ or $I_{HCN2,tail}$ has occurred. The kinetic of the activation is the same as in the last pulse of the PT. Experiment 28-11-2005

switch again to high Na^+ solution for a third PT ($n = 8$ experiments). During the first PT, $I_{HCN2,act}$ declines as expected in most cells ($\mu = 0.18$, SD = 0.25). During the subsequent PT in high K^+ solution, $I_{HCN2,act}$ is about ten times higher than the control in ND96 as expected and remains stable. Ultimately after switching to high Na^+ solution, we measure in the first pulse not only a complete recovery of the $I_{HCN2,act}$ in comparison to the first pulse in the first PT, but even a marked increase in $I_{HCN2,act}$ in all cells ($\mu = -1.12$, SD = 1.63), and during this last PT in high Na^+ solution the $I_{HCN2,act}$ decreases dramatically in all cells ($\mu = 0.49$, SD = 0.32) with a clear slowing down of $\tau_{HCN2,act}$.

In the second protocol, we started with a first test pulse in high K^+/low Na^+ solution to have a control $I_{HCN2,act}$. After switching the bath solution to high Na^+/low K^+ solution, we resume with a PT. The $I_{HCN2,act}$ declines during the PT as anticipated ($\mu = 0.58$, SD = 0.19, $n = 8$). Back to high K^+ solution, we perform a last test pulse. This test pulse activates the same $I_{HCN2,act}$ as the very first control and shows not the least correlation with the change during the PT in high Na^+.

Pulse Train with Other Ions

In experiments in ND96, Barium (5 mM) or Manganese (5 mM) or Br-cAMP (0.25 mM) was added, or BAPTA (5 nmol) was injected to evaluate the effect on the decline of $I_{HCN2,act}$. None of these interventions makes any difference.

Pulse Train with Substitution of Na^+ by Li^+

The same decline of $I_{HCN2,act}$ during PT in high sodium solutions occurs when all Na^+ is substituted by Li^+: the amplitude of $I_{HCN2,act}$ and of $I_{HCN2,tail}$ in the test pulse and the decrease of the currents during the PT in the same oocytes are identical in both solutions.

Discussion

Introduction

The expression of HCN2 channels in *X. laevis* oocytes results in two unexpected problems: a clear increase in conductance at rest potentials in correlation with the amount of expression of HCN2 in the cell membrane and a decline of the activated current during a subsequent train of pulses.

In this paper, we report the results of electrophysiological experiments performed on *X. laevis* oocytes expressing mHCN2 channels in conditions as close as possible to physiological conditions. The properties of the HCN2 current, measured in our experiments with techniques and solutions similar to those of other groups, are comparable

as far as the gating mechanism ($V_{1/2}$ and kinetic) and the fully activated current–voltage relation are concerned. For the sake of comparison, we looked in the literature for similar experiments. In only a few papers, experiments have been performed in comparable conditions. Often the HCN2 mRNA was either subjected to deletion of one aminoacid to obtain better expression or part of the glycosylated N-terminal was cut (Chen et al. 2000, 2001a; Decher et al. 2004; Cheng et al. 2007). Many experiments were performed in isotonic K^+-solutions without Ca^{++} (Chen et al. 2001b; Ulens and Tytgat 2001a, b; Yu et al. 2001; Xue and Li 2002; Xue et al. 2002; Azene et al. 2003; Henrikson et al. 2003; Lesso and Li 2003; Qu et al. 2004; Azene et al. 2005a, b; Pian et al. 2007) although it is well known that high K^+-solutions do modify the kinetic as well as the permeability of the HCN channels (Maruoka et al. 1994; Henrikson et al. 2003; Azene et al. 2005b).

1. Permanent Open HCN2 Channels

Permanently open HCN channels have been described in CHO and HEK cells. In oocytes, the existence of this state has indeed been referred also to many papers but calculated by subtraction of the leak current in uninjected oocytes (Chen et al. 2001a).

Observations at Membrane Resting Potential

In general, HCN channels are supposed to be in a closed state at depolarizing potentials with 98 % closed channels at potentials more positive than −40 mV and to open in a time-dependent way at hyperpolarization with an open probability in ND96 of 0.98 at −83 mV. We do not calculate the min-P_{open} by subtracting the mean leak current for reasons we explained in the data analysis paragraph.

The $E_{rest,0}$ in non-injected cells is the reversal potential of the leak channels present in wild oocytes ($E_{leak,0}$). In injected oocytes, the $E_{rest,1}$ shifts from $E_{rest,0}$ to E_{HCN2} in proportion to the amount of HCN2 expression (Fig. 2). This is in accordance with the hypothesis of the presence of permanently open HCN2 channels at membrane resting potentials.

The membrane conductance at resting potential (G_m) depends only on the number and type of open channels in the oocytes membrane at E_{rest} and should not be influenced by the expression of HCN2 channels, if we suppose that these channels are in the closed state at E_{rest}.

Our experiments reveal a statistical relevant increase in $G_{m,1}$ in cells with expression of HCN2 with a large correlation ($r = 0.599$) between $G_{m,1}$ and $G_{HCN2,act}$, a measure for the amount of expression of HCN2 in the membrane. This is an argument in favour of the expression in the membrane of permanently open channels. $G_{m,1}$ is therefore the addition of the leak conductance in cells without expression ($G_{leak,0}$) and the conductance of the newly expressed open channels ($G_{HCN2,po}$): $G_{m,1} = G_{leak,0} + G_{HCN2,po}$ (Ishii et al. 1999; Chen et al. 2001a; Xue and Li 2002; Xue et al. 2002; Decher et al. 2003; Henrikson et al. 2003; Macri and Accili 2004; Azene et al. 2005b; Proenza and Yellen 2006).

Observations at Activation to Hyperpolarizing Potentials

The instantaneous current at the onset of the pulse (I_{inst}) reflects only the current through channels that are open at the holding potential before the pulse (≥ -40 mV) and should not be dependent on the amount of current that will be activated during the hyperpolarizing pulse. Similarly $G_{inst,1}$ should only represent the conductance of the leak channels in the oocytes membrane at the hyperpolarization potential (AP). Nevertheless the large correlation ($r = 0.764$) between $G_{HCN2,act}$ (x) and $G_{inst,1}$ (y) (Fig. 4) indicates that expression of HCN2 channels not only generates time-dependent channels that activate at hyperpolarization but also permanently open channels (po) that increase $G_{inst,1}$ in proportion to the expression. We suppose that the single-channel conductance of permanently open HCN2 channels is identical to the single-channel conductance of the hyperpolarization-activated HCN2 channels (γ_{HCN2}), but at the moment we have no arguments to prove this hypothesis. The linear correlation $G_{inst,1} = a + b \times G_{HCN2,act}$ has an intercept $a = 0.0081$ μS nF^{-1} and a slope $b = 0.132$ (Fig. 4). Because of the clear correlation with $G_{HCN2,act}$, our working hypothesis is that there is expression of new permanently open channels.

Consider $N_{leak,0}$ = the number of leak channels in uninjected oocytes and $N_{HCN2,PO}$ = the number of permanently open HCN2 channels each with their single-channel conductance $\gamma_{leak,0}$ and γ_{HCN2}. Then $G_{inst,1} = (N_{leak,0} \times \gamma_{leak,0} + N_{HCN2,po} \times \gamma_{HCN2})/C_m$ and $G_{HCN2,act} = (N_{HCN2,act} \times \gamma_{HCN2})/C_m$. Without expression, both $N_{HCN2,po}$ and $N_{HCN2,act}$ are zero and $G_{inst,0} = (N_{leak,0} \times \gamma_{leak,0})/C_m$. The regression line $G_{inst,1} = a + b \times G_{HCN2,act}$ yields an estimation of $G_{inst,0}$ for $G_{HCN2,act} = 0$:$G_{inst,0} = 0.0096$ - μS nF^{-1} (see results: no expression of HCN2) corresponds with $a = 0.0081$ μS nF^{-1} from the regression line. On the other hand, we can derive that the slope ($b = N_{HCN2,po}/N_{HCN,act}$) gives an approximation of the ratio of permanently open HCN2 channel versus activated HCN2 channels. With $b = 0.132$ from the regression line in Fig. 4, we calculate that (0.132/1.132) × 100 = 11.7 % of the HCN2 channels are permanently open and 88.3 % are activated HCN2 channels (Chen et al. 2001a) have for WT ntHCN2 channels a min-P_o at 0.08 ± 0.002 ($n = 8$).

From the regression line $I_{inst,1} = a + b \times I_{HCN2,act}$, we calculate also that $(0.148/1.148) \times 100 = 12.9$ % of all expressed HCN2 channels are permanently open.

This is in favour for our argument that expression not only generates hyperpolarization-activated HCN2 channels but also a fraction of permanently open HCN2 channels.

Observations After Addition of CsCl 2 mM to the Bath Solution

CsCl induces a voltage-dependent block of the HCN2 channel (DiFrancesco 1982). In our experimental conditions, CsCl causes a drop in $G_{m,1}$ proportional to the amount of expression measured before the addition of CsCl but only a fraction of these channels are blocked by Cs^+: ΔGm, $1 = 0.37$ (SD $= 0.20$, $n = 57$). The $i_{inst,1}$ and the corresponding $G_{inst,1}$ also decrease in the same range. These observations agree with the hypothesis that expression of HCN2 induces permanently open channels that are partly sensitive to Cs^+ (Proenza et al. 2002a, b for expression in CHO cells).

Considerations About the Results

It is known that the plasma membrane of *X. laevis* oocytes contains silent ion channels (Tzounopoulos et al. 1995; Schmieder et al. 1998; Sha et al. 2001) and it may be that the injection of mRNA coding for HCN2 activates these intrinsically present channels and induces endogenous currents in the membrane. This possibility is refuted later in the discussion (see: Possible causes of the decline of i_{HCN2}).

An important argument in favour of expression of permanently open HCN2 channels is the effect of Cs^+ on the conductance at rest. Although Cs^+ acts more at potentials more negative than −50 mV (DiFrancesco 1982), we see an effect of the addition of Cs^+ to the bath solution even at less negative potentials.

In the papers published by Sanguinetti's group, there are many instances where the open probability of the HCN2 channel is significant: Figure 3 in Chen et al. 2000 for control ntHCN2 (N-truncated) and Fig. 4 in Chen et al. 2000 where basic residues in the S4 domain are neutralised. The same steady-state open state of ntHCN2, min-P_0, is observed in control: min-P_0 is 0.08 ± 0.02 ($n = 8$), and permanently open ntHCN2 channels are measured after substitution of the aromatic residue at position 331 (Figures 2 in Chen et al. 2001a) as well as by mutation of single residues at position 324 and 339 (Figures 3 and 4 in Chen et al. 2001a). Likewise, a significant min-P_0 is observed when HCN1 currents are measured in oocytes (Figures 3 and 5 in Xue and Li 2002; Figures 2, 3 and 7 in Henrikson et al. 2003; Figure 2 in Azene et al. 2003 and Figs. 3, 7 and 9 in Azene et al. 2005a).

Our observations are in agreement with those of others and indicate that part of the HCN1 and HCN2 channels stay open at potentials positive to –30 mV. This is not observed in wild-type HCN current in SA node cells, cardiac Purkinje fibres or DRG neurons.

2. Use-Dependent Decline in Activated HCN2 Current

A surprising finding during a train of pulses was the unexpected apparent use-dependent decline of the peak activated I_{HCN2} measured both during the hyperpolarizing voltage step and at depolarization. Although it does not happen in all cells and not with the same intensity, we cannot neglect the phenomenon.

These Results are Not Artefacts

(1) As far as the nature of the mRNA injected into the oocytes is concerned, the same results were obtained with mHCN2 and mHCN1 (results not shown) obtained from the group of Dr. J. Tytgat (Laboratory of Toxicology, University of Leuven). HCN2 from another source (Dr. A. Labro, Laboratory of molecular biophysics, physiology and pharmacology, University of Antwerp) yields the same results.

(2) The two-electrode voltage clamp technique is not the cause of the observed current changes. Experiments with too little or too much expressed currents were not taken into consideration. In all our experiments, we measure the membrane potential during the pulses and we have a good control of the potential.

(3) A shift to more negative voltages of the steady-state HCN2 activation voltage is unlikely (see Fig. 7) and moreover we used in some experiments very negative voltage steps (−150 mV) to eliminate this possibility.

(4) In experiments where we measured the E_{HCN2} with a fully activated current–voltage relation before and after a pulse train, we did not have a significant difference of this parameter.

(5) Due to the fact that the conductance of HCN channels is very sensible to the amount of K^+-ions in the extracellular solution, the decline in HCN2 current amplitude could be caused by some decrease in K_o^+, a phenomenon known as depletion of K^+-ion concentration in the restricted space of the T-tubules in skeletal muscle (Almers 1972a, b) or intercellular clefts in cardiac Purkinje fibres (Baumgarten and Isenberg 1977; Baumgarten et al. 1977). A restricted space between the vitelline layer and the cellular

membrane of *X. laevis* oocytes has been described (Dick and Dick 1970). Can the decline of G_{HCN2} in ND96 be the consequence of K^+ depletion?

(a) At hyperpolarizing potentials more negative than E_{Nernst} of K^+ (in ND96 $E_K = -101.8$ mV), the current is essentially an inward Na^+ flux but the small inward flux of K^+ could lower the concentration of K^+_{out} in the restricted space around the membrane especially in cells with great expression and subsequently large currents. During a PT in these conditions, one can expect the $I_{HCN2,act}$ to decline. At depolarizing potentials (−40 to +40 mV), the $I_{HCN2,tail}$ is the sum of an inward Na^+ flux and an outward K^+ flux which may partially or completely restore the depletion of K^+, especially with positive DP. Nevertheless, in PT protocols with positive DP (+40 mV) the G_{HCN2} decreases still.

(b) With hyperpolarizing potentials less negative than E_{Nernst} of K^+ this effect should not happen as the flux of K^+ is always outward. In experiments with AP less negative than E_{Nernst} of K^+ (AP between −101 and −90 mV) the G_{HCN2} declines also.

(c) The effect of lower K^+ in the restricted space on the outside of the membrane should be entirely reversible after restoration of the initial K^+ concentration by diffusion from the bulk solution through the vitelline layer during a long resting period. This is not the case: there is no recuperation of G_{HCN2} in a test pulse after a long period at resting membrane potential in the same solution.

(d) The changes of the HCN2 currents due to depletion should be similar during activation and deactivation, but the changes of $I_{HCN2,act}$ are not simultaneous with the changes of $I_{HCN2,tail}$.

(e) Even oocytes deprived of the vitelline layer show the reduction in $I_{HCN2,act}$.

(6) Run-down of voltage-activated channels in isolated myocytes using whole cell patch clamp technique, in CHO and HEK293 cells expressing various voltage activated channels, is a well known phenomenon (Byerly and Yazejian 1986; Belles et al. 1988; DiFrancesco et al. 1986). This run-down is a consequence of improper control of intracellular calcium, dilution of cytoplasmic ATP and cAMP as well as endogenous PIP_2 (Pian et al. 2006). This run-down has not been described in isolated cells impaled with microelectrodes (Isenberg and Klockner 1982; Hescheler et al. 1982; Callewaert et al. 1984). As far as *X. laevis* oocytes impaled with two microelectrodes are concerned, the only presumably change in cytoplasmic solution is an increase in potassium and chloride concentrations due to electrodiffusion of these ions from the microelectrode filling solutions. The volume of these oocytes compared to single cells is at least two orders of magnitude larger compared to isolated cells, and even if massive influx of KCl takes place, the changes in Ca^{++}, ATP, cAMP and eventually PIP_2 are presumably negligible. We never observed oocyte volume increases that could be the consequence of osmotic influx of H_2O as described in single cells. Anyway, a rundown of the HCN2 current is not present in our experiments because the current is fully restored when the extracellular high Na^+/low K^+ solution is replaced by a high K^+/low Na^+ bath solution.

Possible Cause of the Decline of i_{HCN2}

The progressive activation of an outward current overlapping with the inward current could explain these results. One possible candidate is the Ca^{++}-activated chloride current present in oocytes (Miledi 1982; Barish 1983; Miledi and Parker 1984; Kuruma et al. 2000; Jentsch et al. 2002; Hartzell et al. 2005). At potentials negative to the E_{Cl} of −26 mV, the activation of a Cl^- current could result in an outward flux of Cl^-, thus an inward current. This should increase the total amount of inward current measured during the voltage steps to −120 mV. This is opposite to what we observed. Experiments with intracellular BAPTA, to buffer the intracellular Ca^{++} activity, yielded identical results as those without BAPTA. The activation of an outward K^+ current overlapping with the inward HCN2 current at potentials positive to E_K should be constant during PT and small. In the presence of extracellular Ba^{++}, a blocker of K^+ currents, the decline of I_{HCN2} was still present.

Hypothesis: Change in Ionic Conductances

The decline in activated HCN2 current is presumably the consequence of a reduction in conductance of the channel (Fig. 8). The HCN2 current can be seen as the sum of a Na^+ and a K^+ component: $I_{HCN2} = N_{HCN2} \times P_o \times \gamma_{Na} \times (E - E_{Na}) + N_{HCN2} \times P_o \times \gamma_K \times (E - E_K)$. We state that the voltage-dependent opening probability (P_o) is not affected (Fig. 7), that the density of HCN2 channels

(N_{HCN2}) is not altered (no run down, reversibility of decline in high K^+) and that the ion fluxes during a PT can hardly affect the E_{Nernst} of these ions, so we are left with γ_{Na} and γ_K, the intrinsic conductances of the HCN2 channel that could decline, use-dependently, during a voltage clamp pulse train. These changes occur during the flow of ions through the open HCN2 channel.

A seemingly paradoxical observation is that, during a PT, the amplitude of the changes in I_{HCN2} and the kinetic of these changes are not parallel during activation and deactivation and that the changes are markedly larger in high Na^+ solution than in high K^+ solutions. It may be useful to stress that the fluxes of the permeating ions K^+ and Na^+ are very different during activation and deactivation. During a PT in high Na^+, the $I_{HCN2,act}$ is mainly composed by an inward Na^+ flux because E_{Na} (+58 mV) is largely positive relative to the clamp potential compared to E_K (−102 mV) and the $I_{HCN2,tail}$ is the result of an inward Na^+ and an outward K^+ flux. We hypothesise that the ratio of fluxes of the permeating ions (i_{Na} and i_K) through the channel's selectivity filter could change the conductances of these ions. So the mere passage of much Na^+ through the channel binding with a blocking site within the channel and competing with K^+ ions could change both γ_{Na} and γ_K but it may be that these changes are not simultaneous and not equal in size. In line with our results, we think that a large flux of Na^+ through the channel lowers the conductance for both ions and that a large flux of K^+ enhances rapidly the conductance. This blocking site is not located at the outside of the channel, like the hypothetical K^+ modulating site (DiFrancesco 1982; Frace et al. 1992; Won-Kyung et al. 1994), otherwise the effect of Na^+ would be an instantaneous block like that of Cs^+ (DiFrancesco 1982, 1986; Gauss et al. 1998; Ludwig et al. 1998; Santoro et al. 1998). The process of conductance changes could be caused by the mere presence of Na^+ in a channel where Na^+ and K^+ are competitive and where the Na^+ ion has an inhibiting effect on the channel conductances both for Na^+ and K^+. The block by Na^+ of the HCN2 channel is completely suppressed by K^+ ions after change of the external solution to high K^+, resulting from an eventual displacement of the blocking Na^+ ions by permeating K^+ ions.

In ND96 $\gamma_{Na}/\gamma_K = 0.690$ (SD = 0.112, $n = 343$). After a PT, this ratio has not changed but during the PT there can be dramatic changes with first a decrease (rapid decrease of $I_{HCN2,act}$ only) followed by an increase of the ratio γ_{Na}/γ_K (slower decrease of $I_{HCN2,tail}$ essentially). Concurrently the E_{HCN2} follows these changes: first E_{HCN2} shifts toward E_K (more negative) but later in the PT E_{HCN2} shifts toward E_{Na}. This leads us to the idea that during a PT in high Na^+ the γ_{Na} decreases faster. Ultimately γ_{Na} decreases approximately as much as γ_K and E_{HCN2} regains the control value.

To demonstrate this hypothesis, new experiments on the I_{HCN2} channels with inside-out patches with good control of the outside and inside K^+ and Na^+ ion concentrations are necessary. Single-channel conductance measurements at different potentials might also be interesting to explore a voltage-dependent channel conductance (non-linear current–voltage relation). These single-channel experiments are actually extremely difficult due to the low single-channel conductance of the HCN channel in physiological solutions.

Conclusion

The HCN2 channel constructed with HCN2 α subunits and expressed in oocytes shows clearly different properties from what is known in native cells where next to the α subunits there are β subunits and possibly other modulating factors. We focus on experiments mainly in physiological solutions and in solutions with different potassium concentrations. In the scope of the strong evidence of the presence of permanent open HCN2 channels and the dependence of the G_{HCN2} on the ratio of the transfer of the permeating ions through open channels, the relevance of experiments in the study of physiological mechanisms where the α subunit of HCN2 is used in oocytes is questioned.

No animal studies were carried out by the authors for this article.

Acknowledgments We are very grateful to Dr. Steven A. Siegelbaum Ph.D. (Department of Pharmacology, Columbia University, New York) for his generous gift of mBCNG-2 cDNA encoding for the HCN2 channel and to Prof. Jan Tytgat (Laboratory of Toxicology, University of Leuven) for the preparation of the cRNA and the useful teaching of the techniques of surgical removal of ovarian tissue, preparation and injection of the oocytes. Dr. Alain Labro (Molecular biophysics, physiology and pharmacology, University of Antwerp) was so kind to provide us with cRNA from his constructed cDNA of HCN2 channel. We thank him for the many helpful discussions. We gratefully acknowledge the generous support of the Instituut Born-Bunge.

References

Almers W (1972a) Potassium conductance changes in skeletal muscle and the potassium concentration in the transverse tubules. J Physiol 225:33–56

Almers W (1972b) The decline of potassium permeability during extreme hyperpolarization in frog skeletal muscle. J Physiol 225:57–83

Au KW, Siu CW, Lau CP, Tse HF, Li R (2008) Structural and functional determinants in the S5-P region of HCN-encoded pacemaker channels revealed by cysteine-scanning substitutions. Am J Physiol Cell Physiol 294:C136–C144

Azene E, Xue T, Li R (2003) Molecular basis of the effect of potassium on heterologously expressed pacemaker (HCN) channels. J Physiol 547:349–356

Azene E, Sang D, Tsang SY, Li R (2005a) Pore-to-gate coupling of HCN channels revealed by a pore variant that contributes to gating but not permeation. BBRC 327:1131–1142

Azene E, Xue T, Marbán E, Tomaselli G, Li R (2005b) Non-equilibrium behaviour of HCN channels: insights into the role of HCN channels in native and engineered pacemakers. Cardiovasc Res 67:263–273

Barish M (1983) A transient calcium-dependent chloride current in the immature Xenopus oocytes. J Physiol 342:309–325

Baumgarten C, Isenberg G (1977) Depletion and accumulation of potassium in the extracellular clefts of cardiac Purkinje fibres during voltage clamp hyperpolarization and depolarization. Eur J Physiol 368:19–31

Baumgarten C, Isenberg G, McDonald T, Ten Eick R (1977) Depletion and accumulation of potassium in the extracellular clefts of cardiac Purkinje fibers during voltage clamp hyperpolarization and depolarization. Experiments in sodium-free bathing media. J Gen Physiol 70:149–169

Belles B, Malecot C, Hescheler J, Trautwein W (1988) 'Run-down' of the Ca current during whole-cell recordings in guinea pig heart cells: role of phosphorylation and intracellular Ca^{2+}. Pflug Arch 411:353–360

Bois P, Bescond J, Renaudon B, Lenfant J (1996) Mode of action of bradycardic agent, S 16257, on ionic currents of rabbit sinoatrial node cells. Br J Pharmacol 118:1051–1057

BoSmith R, Briggs I, Sturgess N (1993) Inhibitory actions of Zeneca ZD7288 on whole-cell hyperpolarization activated inward current (If) in guinea-pig dissociated sinoatrial node cells. Br J Pharmacol 110:343–349

Brown DD (2004) A tribute to the *Xenopus laevis* oocyte and egg. J Biol Chem 279:45291–45299

Bucchi A, Baruscotti M, DiFrancesco D (2002) Current-dependent block of rabbit sino-atrial node I_f channels by ivabradine. J Gen Physiol 120:1–13

Byerly L, Yazejian B (1986) Intracellular factors for the maintenance of calcium currents in perfused neurones from the snail, *Lymnea stagnalis*. J Physiol (Lond.) 370:631–650

Callewaert G, Carmeliet E, Vereecke J (1984) Single cardiac Purkinje cells: general electrophysiology and voltage-clamp analysis of the pace-maker current. J Physiol 349:643–661

Chen J, Mitcheson J, Lin M, Sanguinetti M (2000) Functional roles of charged residues in the putative voltage sensor of the HCN2 pacemaker channel. J Biol Chem 275:36465–36471

Chen J, Mitcheson J, Tristani-Firouzi M, Lin M, Sanguinetti M (2001a) The S4–S5 linker couples voltage sensing and activation of pacemaker channels. Proc Natl Acad Sci USA 98: 11277–11282

Chen S, Wang J, Siegelbaum S (2001b) Properties of hyperpolarization-activated current defined by coassembly of HCN1 and HCN2 subunits and basal modulation by cyclic nucleotide. J Gen Physiol 117:491–503

Cheng L, Kinard K, Rajamani R, Sanguinetti M (2007) Molecular mapping of the binding site for a blocker of hyperpolarization-activated, cyclic nucleotide-modulated pacemaker channels. JPET 322:931–939

Colville C, Gould G (1994). Expression of membrane transport proteins in Xenopus oocytes. In: Membrane protein expression systems: A User's Guide, ed. Gould G, pp. 243–274. Portland Press, London

Costa PF, Emilio MG, Fernandes PL, Ferreira HG, Ferreira KG (1989) Determination of ionic permeability coefficients of the plasma membrane of *Xenopus laevis* oocytes under voltage clamp. J Physiol 413:199–211

Dascal N (1987) The use of Xenopus oocytes for the study of ion channels. Crit Rev Biochem Mol Biol 22:317–387

Decher N, Bundis F, Vajna R, Steinmeyer K (2003) KCNE2 modulates current amplitudes and activation kinetics of HCN4: influence of KCNE family members on HCN4 currents. Eur J Physiol 446:633–640

Decher N, Chen J, Sanguinetti M (2004) Voltage-dependent gating of hyperpolarization-activated, cyclic nucleotide-gated pacemaker channels. J Biol Chem 279:13859–13865

Deitmer J, Ellis D (1980) Interactions between the regulation of the intracellular pH and sodium activity of sheep cardiac Purkinje fibres. J Physiol 304:471–488

Dick E, Dick D (1970) The effect of surface microvilli on the water permeability of single toad oocytes. J Cell Sci 6:454–476

Dick D, McLaughlin S (1969) The activities and concentrations of sodium and potassium in toad oocytes. J Physiol 205:61–78

DiFrancesco D (1982) Block and activation of the pace-maker channel in calf Purkinje fibres: effects of potassium, caesium and rubidium. J Physiol 329:485–507

DiFrancesco D (1985) The cardiac hyperpolarizing-activated current, i_f. Origins and developments. Prog Biophys Mol Biol 46: 163–183

DiFrancesco D (1986) Characterization of single pacemaker channels in cardiac sino-atrial node cells. Nature 324:470–473

DiFrancesco D (1994) Some properties of the UL-FS 49 block of the hyperpolarization-activated current (i_f) in sino-atrial node myocytes. Eur J Physiol 427:64–70

DiFrancesco D, Ferroni A, Mazzanti M, Tromba C (1986) Properties of the hyperpolarizing-activated current (i_f) in cells isolated from the rabbit sino-atrial node. J Physiol 377:61–88

Eidne K (1994). Expression of receptors in Xenopus oocytes. In: Membrane protein expression systems: A User's Guide, ed. Gould G, pp 275–299. Portland Press, London

Frace A, Maruoka F, Noma A (1992) Control of the hyperpolarization-activated cation current by external anions in rabbit sino-atrial node cells. J Physiol 453:307–318

Gauss R, Seifert R, Kaupp B (1998) Molecular identification of a hyperpolarization-activated channel in sea urchin sperm. Nature 393:583–587

Goethals M, Raes A, Van Bogaert PP (1993) Use-dependent block of the pacemaker current I_f in rabbit sinoatrial node cells by Zatebradine. Circulation 88:2389–2401

Hartzell C, Putzier I, Arreola J (2005) Calcium-activated chloride channels. Annu Rev Physiol 67:719–758

Henrikson C, Xue T, Dong P, Sang D, Marban E, Li R (2003) Identification of a surface charged residue in the S3-S4 linker of the pacemaker (HCN) channel that influences activation gating. J Biol Chem 278:13647–13654

Hescheler J, Pelzer D, Trube G, Trautwein W (1982) Does the organic channel blocker D600 act from inside or outside on the cardiac cell membrane? Pflüg Arch 393:287–291

Hestrin S (1987) The properties and function of inward rectification in rod photoreceptors of tiger salamander. J Physiol 390:319–333

Isenberg G, Klockner U (1982) Isolated bovine ventricular myocytes. Characterization of the action potential. Pflug Arch 395:19–29

Ishii T, Takano M, Xie LH, Noma A, Ohmori H (1999) Molecular characterization of the hyperpolarization-activated cation channel in rabbit heart sinoatrial node. J Biol Chem 274: 12835–12839

Jentsch T, Stein V, Weinreich F, Zdebik A (2002) Molecular structure and physiological function of chloride channels. Phys Rev 82:503–568

Kuruma A, Hirayama Y, Hartzell C (2000) A hyperpolarization- and acid-activated nonselective cation current in Xenopus oocytes. AJP 279:C1401–C1413

Lesso H, Li R (2003) Helical secondary structure of the external S3-S4 linker of pacemaker (HCN) channels revealed by site-

dependent perturbations of activation phenotype. J Biol Chem 278:22290–22297

Ludwig A, Zong X, Jeglitsch M, Hofmann F, Biel M (1998) A family of hyperpolarization-activated mammalian cation channels. Nature 393:587–591

Macri V, Accili E (2004) Structural elements of instantaneous and slow gating in hyperpolarization-activated cyclic nucleotide-gated channels. J Biol Chem 279:16832–16846

Macri V, Proenza C, Agranovich E, Angoli D, Accili E (2002) Separable gating mechanisms in a mammalian pacemaker channel. J Biol Chem 277:35939–35946

Maruoka F, Nakashima Y, Takano M, Ono K, Noma A (1994) Cation-dependent gating of the hyperpolarization-activated cation current in the rabbit sino-atrial node cells. J Physiol 477:423–435

Miledi R (1982) A calcium-dependent transient outward current in *Xenopus laevis* oocytes. Proc R Soc Lond B 215:491–497

Miledi R, Parker I (1984) Chloride current induced by injection of calcium into Xenopus oocytes. J Physiol 357:173–183

Moroni A, Barbuti A, Altomare C, Viscomi C, Morgan J, Baruscotti M, DiFrancesco D (2000) Kinetic and ionic properties of human HCN2 pacemaker channel. Eur J Physiol 439:618–626

Pian P, Bucchi A, Robinson R, Siegelbaum S (2006) Regulation of gating and rundown of HCN hyperpolarization-activated channels by exogenous and endogenous PIP_2. J Gen Physiol 128:593–604

Pian P, Bucchi A, DeCostanzo A, Robinson R, Siegelbaum S (2007) Modulation of cyclic nucleotide-regulated HCN channels by PIP_2 and receptors coupled to phospholipase C. Eur J Physiol 455:125–145

Proenza C, Yellen G (2006) Distinct populations of HCN pacemaker channels produce voltage-dependent and voltage-independent currents. J Gen Physiol 127:183–190

Proenza C, Angoli D, Agranovich E, Macri V, Accili EA (2002a) Pacemaker channels produce an instantaneous current. J Biol Chem 277:5101–5109

Proenza C, Tran N, Angoli D, Zahynacz K, Balcar P, Accili E (2002b) Different roles for the cyclic nucleotide binding domain and amino terminus in assembly and expression of hyperpolarization-activated, cyclic nucleotide-gated channels. J Biol Chem 277:29634–29642

Qu J, Kryukova Y, Potapova I, Doronin S, Larsen M, Krishnamurthy G, Cohen I, Robinson R (2004) MiRP1 modulates HCN2 channel expression and gating in cardiac myocytes. J Biol Chem 279:43497–43502

Raes A, Van De Vijver G, Goethals M, Van Bogaert PP (1998) Use-dependent block of I_h in mouse dorsal root ganglion neurons by sinus node inhibitors. Br J Pharmacol 125:741–750

Santoro B, Liu D, Yao H, Barsch D, Kandel E, Siegelbaum S, Tibbs G (1998) Identification of a gene encoding a hyperpolarization-activated pacemaker channel of brain. Cell 93:717–729

Schmieder S, Lindenthal S, Banderali U, Ehrenfeld J (1998) Characterization of the putative chloride channel xClC-5 expressed in *Xenopus laevis* oocytes and comparison with endogenous chloride currents. J Physiol 511(2):379–393

Sha Q, Lansbery K, Distefano D, Mercer R, Nichols C (2001) Heterologous expression of the Na^+, K^+-ATPase γsubunit in Xenopus oocytes induces an endogenous, voltage-gated large diameter pore. J Physiol 535(2):407–417

Smart TG, Krishek BJ (1995). Xenopus oocyte microinjection and ion-channel expression. In: Patch-clamp applications and protocols, ed. Boulton A, Baker G & Waltz W, pp. 259–305. Humana Press, New York

Stamps P, Begenisich T (1998) Unidirectional fluxes through ion channels expressed in Xenopus oocytes. Methods Enzymol 293:556–564

Stieber J, Wieland K, Stöckl G, Ludwig A, Hofman F (2006) Bradycardic and proarrhythmic properties of sinus node inhibitors. Mol Pharmacol 69:1328–1337

Thollon C, Bedut S, Villeneuve N, Cogé F, Piffard L, Guillaumin JP, Brunel-Jacquemin C, Chomarat P, Boutin JA, Peglion JL, Vilaine JP (2007) Use-dependent inhibition of hHCN4 by ivabradine and relationship with reduction in pacemaker activity. Br J Pharmacol 150:37–46

Tzounopoulos T, Maylie J, Adelman JP (1995) Induction of endogenous channels by high levels of heterologous membrane proteins in *Xenopus* Oocytes. Biophys J 69:904–908

Ulens C, Tytgat J (2001a) Functional heteromerization of HCN1 and HCN2 pacemaker channels. J Biol Chem 276:6069–6072

Ulens C, Tytgat J (2001b) G_i- and G_S-coupled receptors up regulate the cAMP cascade to modulate HCN2, but not HCN1 pacemaker channels. Eur J Physiol 442:928–942

Van Bogaert PP, Goethals M (1987) Pharmacological influence of specific bradycardic agents on the pacemaker current of sheep cardiac Purkinje fibres. A comparison between three different molecules. Eur Heart J 8:L35–L42

Van Bogaert PP, Goethals M, Simoens C (1990) Use- and frequency-dependent blockade by UL-FS 49 of the i_f pacemaker current in sheep cardiac Purkinje fibres. Eur J Pharmacol 187:241–256

Van Bogaert PP, Pittoors F (2003) Use-dependent blockade of cardiac pacemaker current (If) by cilobradine and zatebradine. Eur J Pharmacol 478:161–171

Weber W (1999) Ion currents of Xenopus laevis oocytes: state of the art. Biochim Biophys Acta 1421:213–233

Won-Kyung H, Brown H, Noble D (1994) High selectivity of the i_f channel to Na^+ and K^+ in rabbit isolated sinoatrial node cells. Eur J Physiol 426:68–74

Xue T, Li R (2002) An external determinant in the S5-P linker of the pacemaker (HCN) channel identified by sulfhydril modification. J Biol Chem 277:46233–46242

Xue T, Marbán E, Li R (2002) Dominant-negative suppression of HCN1- and HCN2-encoded pacemaker currents by an engineered HCN1 construct. Circ Res 90:1267–1273

Yu H, Wu J, Potapova I, Wymore R, Holmes B, Zuckerman J, Pan Z, Wang H, Shi W, Robinson R, El-Maghrabi M, Benjamin W, Dixon J, McKinnon D, Cohen I, Wymore R (2001) MinK-Related Peptide 1. A β subunit for the HCN ion channel subunit family enhances expression and speeds activation. Circ Res 88:e84–e87